KASCADE-Grande observation of features in the cosmic ray spectrum between knee and ankle

2013 J. Phys.: Conf. Ser. 409 012005

DOI: 10.1088/1742-6596/409/1/012005

KASCADE-Grande observation of features in the cosmic ray spectrum between knee and ankle

2013 J. Phys.: Conf. Ser. 409 012005

(http://iopscience.iop.org/1742-6596/409/1/012005)

Journal of Physics: Conference Series **409** (2013) 012005 doi:10.1088/1742-6596/409/1/012005

KASCADE-Grande observation of features in the cosmic ray spectrum between knee and ankle

A Haungs[1], W D Apel[1], J C Arteaga-Velázquez[2], K Bekk[1], M Bertaina[3], J Blümer[1,4], H Bozdog[1], I M Brancus[5], E Cantoni[3,6], A Chiavassa[3], F Cossavella[4,a], K Daumiller[1], V de Souza[7], F Di Pierro[3], P Doll[1], R Engel[1], J Engler[1], M Finger[4], B Fuchs[4], D Fuhrmann[8], H J Gils[1], R Glasstetter[8], C Grupen[9], D Heck[1], J R Hörandel[10], D Huber[4], T Huege[1], K-H Kampert[8], D Kang[4], H O Klages[1], K Link[4], P Łuczak[11], M Ludwig[4], H J Mathes[1], H J Mayer[1], M Melissas[4], J Milke[1], C Morello[6], J Oehlschläger[1], S Ostapchenko[1,b], N Palmieri[4], M Petcu[5], T Pierog[1], H Rebel[1], M Roth[1], H Schieler[1], S Schoo[4], F Schröder[1], O Sima[12], G Toma[5], G C Trinchero[6], H Ulrich[1], A Weindl[1], J Wochele[1], M Wommer[1], J Zabierowski[11]

[1] Institut für Kernphysik, KIT - Karlsruher Institut für Technologie, Germany
[2] Universidad Michoacana, Instituto de Fisica y Matemáticas, Morelia, Mexico
[3] Dipartimento di Fisica, Università degli Studi di Torino, Italy
[4] Institut für Experimentelle Kernphysik, KIT - Karlsruher Institut für Technologie, Germany
[5] National Institute of Physics and Nuclear Engineering, Bucharest, Romania
[6] Osservatorio Astrofisico di Torino, INAF Torino, Italy
[7] Universidade São Paulo, Instituto de Física de São Carlos, Brasil
[8] Fachbereich Physik, Universität Wuppertal, Germany
[9] Fachbereich Physik, Universität Siegen, Germany
[10] Dept. of Astrophysics, Radboud University Nijmegen, The Netherlands
[11] National Centre for Nuclear Research, Department of Cosmic Ray Physics Łódź, Poland
[12] Department of Physics, University of Bucharest, Bucharest, Romania
[a] now at: Max-Planck-Institut für Physik, München, Germany
[b] now at: University of Trondheim, Norway

E-mail: haungs@kit.edu

Abstract. The detection of high-energy cosmic rays above a few hundred TeV is realized by the observation of extensive air-showers. By using the multi-detector setup of KASCADE-Grande, and here in particular the detectors of the large Grande array, the energy spectrum and the elemental composition of high-energy cosmic rays in the energy range from 10 PeV to 1 EeV are investigated. The estimation of energy and mass of the high-energy primary particles is based on the combined analysis of the total number of charged particles and the total number of muons measured by the detector arrays of Grande and KASCADE, respectively. The latest analysis results have shown that in the all-particle spectrum two features are present: a hardening of the spectrum at energies around 20 PeV and a steepening, i.e. a knee-like structure, at 80-90 PeV. The latter one was found to be due to a decrease of flux of the heavy mass component.

1. Introduction

What are the source and the acceleration mechanism of galactic cosmic rays and at which energy, if at any, appears the transition to extragalactic origin of cosmic rays? This basic question in astroparticle physics still wait for a conclusive answer. Possible scenarios range from supernova remnants (SNR) [1], superbubbles [2] and magnetars [3] to cannonballs from supernovae [4] and the remnants of gamma-ray bursts in our galaxy [5], being the SNR model the most accepted paradigm. All these models have in common that they predict the existence of individual knee-like structures or breaks in the corresponding spectra of cosmic nuclei, which are associated with the efficiency of the accelerator or features of the particle propagation through the Galaxy. Such structures lead to the formation of a knee at around $3 - 5 \cdot 10^{15}$ eV in the all-particle energy spectrum, which is a prominent feature discovered in the cosmic ray flux caused by a steepening of the spectrum [6]. According to most theories, the positions of the knees are distributed inside the energy interval from $E = 10^{15}$ to 10^{17} eV and scale with the electric charge, Z, of the ion ($E_Z \propto Z \times B \times R$, with B: the magnitude of the magnetic field and R: the size of the confinement region). Consequently, cosmic rays of higher energies than the break of the heaviest primaries with considerable abundance in the flux, should predominantly originate from extragalactic sources.

Some clues to elucidate among the different models are to be found in the study of the properties of cosmic rays, i.e., the analysis of their energies, arrival directions and composition. Measurements performed by the KASCADE experiment in the energy range $E = 10^{15} - 10^{17}$ eV revealed in fact the existence of individual knees in the spectra of the light and intermediate mass groups of cosmic rays ($Z \leq 14$) [7], which was confirmed by subsequent observations from other experiments. KASCADE also discovered that the individual breaks observed in the energy spectra of the light mass groups ($Z < 6$) were the origin of the knee feature of the all-particle cosmic ray flux, which KASCADE assigns to $E = 4 - 5.7 \cdot 10^{15}$ eV [7]. From the results of the experiment a pattern emerged, in which the positions of the individual knees are shifted to higher energies as the atomic number of the primaries increases. However, these data are not enough to rule out a Z- or A- dependence of the individual knees due to the uncertainties in the measured locations of the breaks. A convincing argument in favor of one or another type of dependence would come from the measurement of the knee of the heavy mass group (for which Fe is the representative element). That structure was missing in the KASCADE data, presumably due to the lack of statistics at the energies of interest. Assuming $E_H \approx (2 - 3) \cdot 10^{15}$ eV [7] for the position of the knee of the hydrogen mass group of cosmic rays, then the break for iron nuclei is expected at energies in the interval $E_{Fe} = (Z \cdot E_H, A \cdot E_H) \approx (7 \cdot 10^{16}\,\text{eV}, 1.7 \cdot 10^{17}\,\text{eV})$, outside the sensitivity range of the KASCADE experiment. To explore this energy regime in search for the so called iron-knee, KASCADE was extended to KASCADE-Grande [8] using the components of the EAS-TOP observatory [9]. During the period from 2003 to 2011, measurements of cosmic ray events were performed with KASCADE-Grande in the interval $10^{16} - 10^{18}$ eV and first results from different analyses concerning the all-particle energy spectrum and the composition of the light and heavy components of galactic cosmic rays were released during 2010 and 2011 [10–13]. In this contribution, we will take a fast look into the KASCADE-Grande instrument and will sum up the details of the analyses on spectral features in this energy range and their main results.

2. KASCADE-Grande

Main parts of the experiment are the Grande array, spread over an area of $700 \times 700\,\text{m}^2$, the original KASCADE array, covering $200 \times 200\,\text{m}^2$ with unshielded and shielded detectors, and additional muon tracking devices. This multi-detector system allows us to investigate the energy spectrum, composition, and anisotropies of cosmic rays in the energy range up to 1 EeV. The estimation of energy and mass of the primary particles is based on the combined investigation

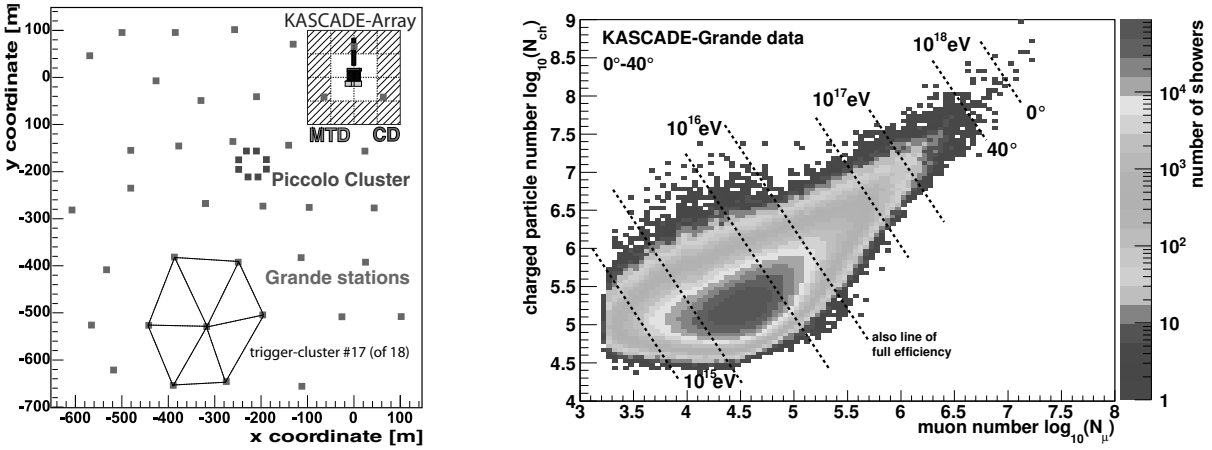

Figure 1. Left: Layout of the KASCADE-Grande experiment: The original KASCADE (with Array, Muon Tracking Detector and Central Detector), the distribution of the 37 stations of the Grande array, and the small Piccolo cluster for fast trigger purposes are shown. The outer 12 clusters of the KASCADE array consist of μ- and e/γ-detectors, the inner 4 clusters of e/γ-detectors, only.
Right: Two-dimensional distribution of the shower sizes: charged particle number and total muon number as measured by KASCADE-Grande. All quality cuts are applied, i.e. these data are the basis for the energy reconstruction and the mass composition studies.

of the charged particle, the electron, and the muon components measured by the detector arrays of Grande and KASCADE.

The multi-detector experiment KASCADE [14] (located at 49.1°n, 8.4°e, 110 m a.s.l.) was extended to KASCADE-Grande in 2003 by installing a large array of 37 stations consisting of $10\,\mathrm{m}^2$ scintillation detectors each (fig. 1). KASCADE-Grande [8] provides an area of $0.5\,\mathrm{km}^2$ and operates jointly with the existing KASCADE detectors. The joint measurements with the KASCADE muon tracking devices are ensured by an additional cluster (Piccolo) located close to the center of KASCADE-Grande and deployed for fast trigger purposes. For results of the muon tracking devices see references [11]. While the Grande detectors are sensitive to charged particles, the KASCADE array detectors measure the electromagnetic component and the muonic component separately. These muon detectors enable to reconstruct the total number of muons on an event-by-event basis also for Grande triggered events.

Basic shower observables like the core position, angle-of-incidence, and total number of charged particles are provided by the measurements of the Grande stations. A core position resolution of $\approx 5\,\mathrm{m}$, a direction resolution of $\approx 0.7°$, and a resolution of the total particle number in the showers of $\approx 15\%$ is achieved. The total number of muons (N_μ resolution $\approx 25\%$) is calculated using the core position determined by the Grande array and the muon densities measured by the KASCADE muon array detectors. Full efficiency for triggering and reconstruction of air-showers is reached at a primary energy of $\approx 10^{16}\,\mathrm{eV}$, slightly varying on the cuts needed for the reconstruction of the different observables [8].

The strategy of the KASCADE-Grande data analysis to reconstruct the energy spectrum and elemental composition of cosmic rays is to use the multi-detector set-up of the experiment and to apply different analysis methods to the same data sample. This has advantages in various aspects. One would expect the same results by all methods when the measurements are accurate enough, when the reconstructions work without failures, and when the Monte-Carlo simulations

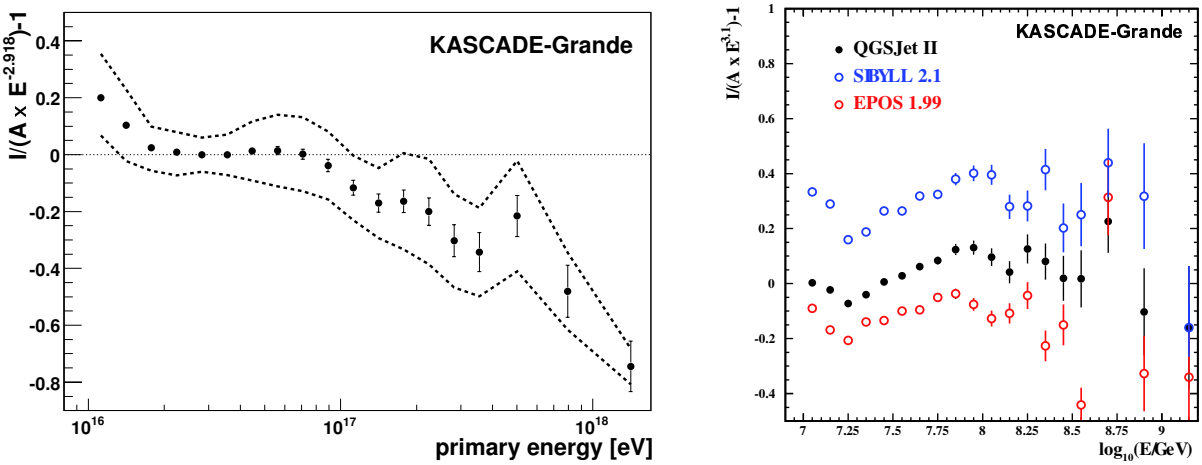

Figure 2. Left: The all-particle energy spectrum obtained with KASCADE-Grande. The residual intensity after multiplying the spectrum with a factor of $E^{2.918}$ and normalized with A is displayed as well as the band of systematic uncertainty [13].
Right: These spectra are obtained by the same procedure applied to the data as shown in the left panel (without the unfolding procedure), but now the calibration is based on three different hadronic interaction models.

describe correctly and consistently the shower development and detector response [13].

The main air-shower observables of KASCADE-Grande, shower size and total number of muons, could be reconstructed with high precision and low systematic uncertainties and are used in the following for the data analysis (fig. 1, right panel).

3. The all-particle energy spectrum

In a first step of the analysis, we reconstructed the all-particle energy spectrum. Applying various reconstruction methods to the KASCADE-Grande data the obtained all-particle energy spectra are compared for cross-checks of the reconstruction, for studies of systematic uncertainties and for testing the validity of the underlying hadronic interaction models. By combining both observables and using the hadronic interaction model QGSJet-II [15], a composition independent all-particle energy spectrum of cosmic rays is reconstructed in the energy range of 10^{16} eV to 10^{18} eV within a total systematic uncertainty in flux of 10-15% [13]. To obtain the all-particle spectrum an unfolding procedure was applied to correct for effects on the steeply falling spectrum by reconstruction uncertainties.

Despite the overall smooth power-law behavior of the resulting all-particle spectrum, there are some structures observed, which do not allow to describe the spectrum with a single slope index [13].

Just above 10^{16} eV the spectrum exhibits a concave behavior, which is significant with respect to the systematic and statistical uncertainties. This is true despite the fact that only vertical showers contribute to the spectrum in this energy range. This hardening of the spectrum is validated by several cross-checks, e.g., by efficiency correction of more inclined events based on simulations. A hardening of the spectrum is expected, e.g. when a pure rigidity dependence of the galactic cosmic rays is assumed. Depending on the relative abundances of the different primaries one would expect charge dependent steps (i.e. slope changes) in the all-particle spectrum. But, on the other hand, there are also other possible astrophysical scenarios to get a concave behavior of the cosmic ray spectrum. In general, a transition from one source population to another one

could also result in a hardening of the spectrum.

Another feature in the spectrum is constituted by a small break at around $8 \cdot 10^{16}$ eV. The power law index of $\gamma = -2.95 \pm 0.05$ is obtained by fitting the range before this break. Applying a second power law above the break an index of $\gamma = -3.24 \pm 0.08$ is obtained (see figure 2). With a statistical significance of more than 2 sigma the two power laws are incompatible with each other. This slight slope change occurs at an energy where the rigidity dependent knee of the iron component would be expected (KASCADE QGSJet01 based analysis assigns the proton knee to an energy of $2 - 4 \cdot 10^{15}$ eV) [7].

Despite the fact, that the discussed spectrum is based on the QGSJet-II hadronic interaction model, there is confidence that the found structures of the energy spectrum remain stable. The same analysis procedure were performed with EPOS [16] and SIBYLL [17] as hadronic interaction models for the energy calibration. These analyses result in similar structures in the all-particle spectrum, but the spectra are shifted in the energy scale (see fig. 2, right panel). For the all-particle energy spectrum, the flux differences of EPOS 1.99 and SIBYLL 2.1 with respect to QGSJET-II-2 are about 15% and less than 10%, respectively. The spectral shapes are in reasonable agreement for the three interaction models [18]. In addition, investigations of the spectra of the pure (and independently obtained) observables, shower size and total muon number, confirmed the structures [13].

4. Single mass group spectra

A conclusion on the origin of the found structures in the all-particle spectrum is not possible without investigating the composition in detail in this energy range. The basic goal of the KASCADE-Grande experiment is the determination of the chemical composition in the primary energy range $10^{16} - 10^{18}$ eV. Like for the reconstruction of the energy, again several methods using different observables are applied to the registered data in order to study systematic uncertainties. However, the influence of the predictions of the hadronic interaction models has a much larger effect on the composition than on the primary energy. As it is well known from KASCADE data analysis [7] that the relative abundances of the individual elements or elemental groups are very dependent on the hadronic interaction model underlying the analyses, the strategy is to derive the energy spectra of the individual mass groups. The structure or characteristics of these spectra are found to be much less affected by the differences of the various hadronic interaction models than the relative abundance. The present goal is to verify the structure found in the all-particle energy spectrum at around 100 PeV in the individual mass group spectra and to assign it to a particular mass group.

The main observables taken into account for composition studies at KASCADE-Grande are the shower size (N_{ch}, or the subsequently derived electron number N_e) and the muon shower size (N_μ). Figure 1, right panel, displays the correlation of these two observables, i.e. this distribution is the basis of the composition analysis with KASCADE-Grande data. So far, in the composition analysis, we concentrate on interpreting the data with the hadronic interaction model QGSJet-II (and FLUKA as low energy interaction model).

For all the methods, it is crucial to verify the sensitivity of the observables to different primary particles and the reproducibility of the measurements with the hadronic interaction model in use as a function of sizes and the atmospheric depth. Four methods of composition studies at KASCADE-Grande were discussed, all showing the same result: The knee-like structure in the all-particle spectrum at $\approx 8 \cdot 10^{16}\, eV$ is due to the decrease of the flux of the heavy component of primary cosmic particles. One of the methods will be explained in a bit more detail in the following:

Using the above mentioned reconstruction of the energy spectrum by correlating the size of the charged particles N_{ch} and muons N_μ on an event-by-event basis, the mass sensitivity is minimized by means of the parameter $k(N_{ch}, N_\mu)$ [12]. This quantity, generally describing

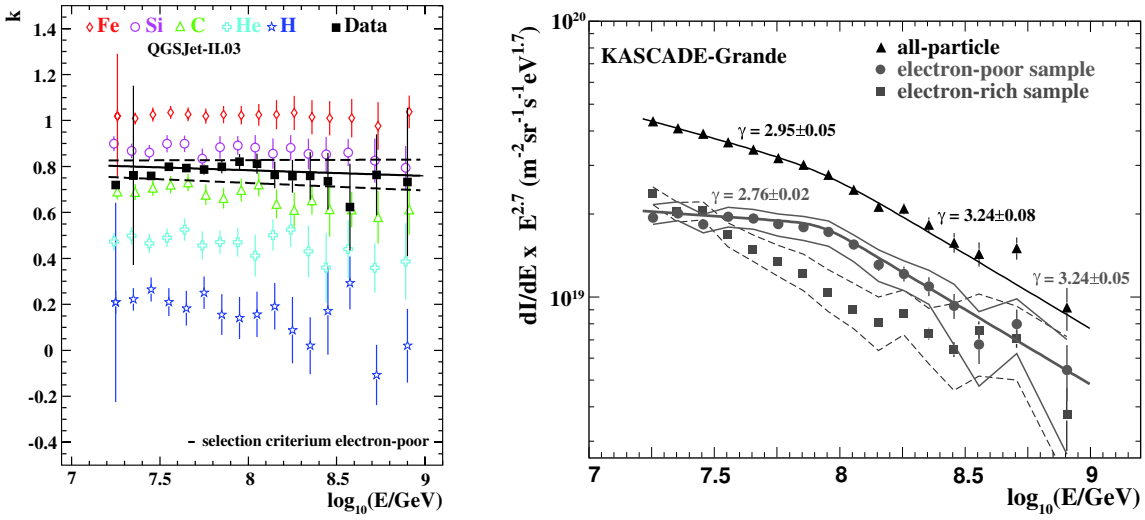

Figure 3. Left: Mean k parameter vs reconstructed energy for different primaries according to MC simulations (CORSIKA/QGSJET II). The full line represent the frontier line used for classification of experimental data into different mass groups and the dashed lines the corresponding uncertainties on this definition. Statistical and reconstruction uncertainties of k are shown as error bars. Right: Reconstructed all-particle energy spectrum together with the spectra of the electron-poor and electron-rich components. Fits on the spectra with a double power-law formula and resulting slopes are also indicated.

the ratio of the total muon number to the shower size (i.e. discriminating electron-rich and electron-poor air showers) is sensitive to the composition of the primary particles (H, He, C, Si, Fe) and can be employed to separate the data into the different mass groups: light and heavy, at least. To achieve the separation, a plot with the mean value of k for different primaries as a function of the reconstructed energy is created from MC simulations for every zenith angle interval into which data is divided. An example, of such a graph can be seen in the left panel of figure 3. It happens that, in general, the mean k value grows with the mass of the particle. That is not surprising, since the k parameter is defined in such a way that it returns the biggest values for iron nuclei and the lowest, for protons. With the above plots, data is divided into two groups by defining the frontier line $\bar{k}_{Si-C}$, obtained from a fit to the average between the mean k values of Si and C. Events with $k > \bar{k}_{Si-C}$ are classified as part of the heavy component. If $k < \bar{k}_{Si-C}$, the events will be part of the light mass group. The energy spectra for the light and heavy mass groups are presented in figure 3 (right panel) along with the all-particle energy spectrum obtained by adding the individual spectra. In this plot, the knee around 10^{17} eV in the all-particle energy spectrum is seen again. But now, its origin is clearer. The answer must be tracked down to the existence of a knee in the energy spectrum of the heavy component, whose relative abundance around 10^{17} eV is bigger than that of the other mass groups. It is worth to mention that the presence of the knee-feature and the existence of not vanishing light mass groups are independent of the high-energy hadronic interaction models. That was checked out by reproducing the analysis within the framework of EPOS 1.99. As the significance of the break of the all-particle spectrum increases significantly when enhancing heavy primaries, it is obvious that this structure is introduced by heavy primaries.

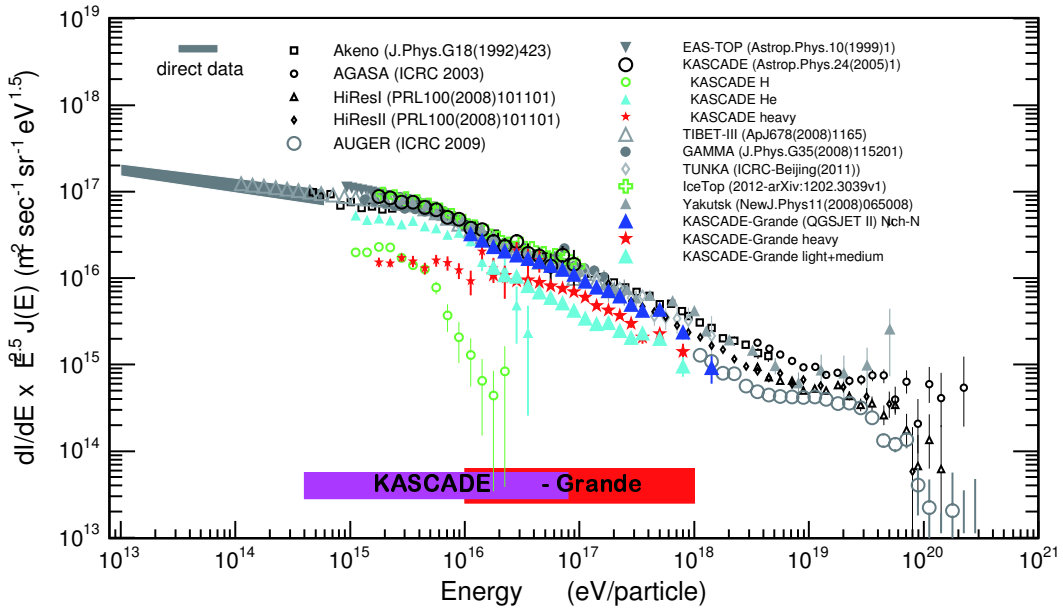

Figure 4. KASCADE and KASCADE-Grande reconstructed energy spectra of individual mass groups.

5. Conclusion

The main conclusions of this research are that the spectrum of the heavy component of cosmic rays exhibits a knee-like feature around $8 \cdot 10^{16}$ eV, which is responsible for a subtle break in the all-particle energy spectrum around the same energy value. For the second structure found within the KASCADE-Grande energy range, the hardening of the all-particle spectrum at $\approx 20\,\mathrm{PeV}$, the composition analysis is still in progress.

The overall experimental situation is compiled in figure 4, where the present KASCADE-Grande results are compared with earlier KASCADE results as well as with the all-particle spectra of various experiments.

It was found that QGSJet-II, the hadronic interaction model in use, can fairly well reproduce the data and, in particular, provides a consistent solution on the elemental composition, independent of the method in use. One has to remark, that using other hadronic interaction models lead to significant changes in the relative abundances of the elemental groups as different models predict different shower sizes for a certain energy and mass of the primary cosmic ray, but we are confident that the obtained spectral form for the heavy and light component of the cosmic ray spectrum remains unchanged.

Acknowledgement: KASCADE-Grande is supported by the BMBF of Germany, the MIUR and INAF of Italy, the Polish Ministry of Science and Higher Education (this work partly by grant for 2009-2011). This work was partially supported by the Romanian Authority for Scientific Research UEFISCDI (PNII-IDEI grants 17/2011 and 271/2011), and the German-Mexican bilateral collaboration grant (DAAD-Proalmex 2009-2012). J.C.A.V. acknowledges the partial support of CONACyT and the Coordinación de la Investigación Científica de la Universidad Michoacana.

References

[1] Ptuskin V S, et al 1993 *A&A* **268** 726
[2] Binns W R, et al 2008 *New Astronomy Reviews* **52** 427
[3] Blasi P, Epstein R L and Olinto A V 2000 *ApJ* **533** L123
[4] De Rújula A 2005 *Nucl. Phys. B, Proc. Suppl.* **151** 23
[5] Wick S D, Dermer C D and Atoyan A 2004 *Astrop. Phys.* **21** 125
[6] Kulikov G V and Khristiansen G B 1959 *Sov. Phys. JETP* **35** 441
[7] Antoni T, et al (KASCADE Collaboration) 2005 *Astrop. Phys.* **24** 1
[8] Apel W D, et al (KASCADE-Grande Collaboration) 2010 *NIM A* **620** 202
[9] Aglietta M, et al (EAS-TOP Collaboration) 2004 *Astrop. Phys.* **21** 583
[10] Bertaina M, et al (KASCADE-Grande Collaboration) 2011 *Astrop. Space Sci. Trans.* **7** 229
[11] Apel W D, et al (KASCADE-Grande Collaboration) 2011 *KASCADE-Grande contributions to the 32nd ICRC, Beijing, China* astro-ph/1111.5436v1
[12] Apel W D, et al (KASCADE-Grande Collaboration) 2011 *PRL* **107** 171104
[13] Apel W D, et al (KASCADE-Grande Collaboration) 2012 *Astropart. Phys.* **36** 183
[14] Antoni T, et al (KASCADE Collaboration) 2003 *NIM A* **513** 429
[15] Ostapchenko S S 2006 *Phys. Rev.* **D 74** 014026
[16] Pierog T, et al 2009 *Rep. Forschungszentrum Karlsruhe* **FZKA 7516** 133
[17] Ahn E J, et al 2009 *Phys. Rev. D* **80** 094003
[18] Kang D, et al (KASCADE-Grande Collaboration) 2012 *ECRS Moscow* these proceedings